quaternary

MDPI

Article

Upper Pleistocene Marine Levels of the Es Copinar–Es Estufadors (Formentera, Balearic Islands, West Mediterranean)

Laura del Valle [1,2,*], Guillem X. Pons [1] and Joan J. Fornós [2]

[1] Geography Department, University of the Balearic Islands, Ctra. de Valldemossa km 7.5, 07121 Palma, Spain; guillemx.pons@uib.es
[2] Earth Science Research Group, University of the Balearic Islands, Ctra. de Valldemossa km 7.5, 07121 Palma, Spain; joan.fornos@uib.es
* Correspondence: laura.del-valle@uib.eu; Tel.: +34-971173183

Abstract

Late Pleistocene coastal deposits on the southeastern coast of Formentera (Es Ram–Es Estufadors) provide a high-resolution record of sea-level and climatic fluctuations associated with Marine Isotope Stage (MIS) 5. Three distinct beach levels (Sef-1, Sef-2, Sef-3) were identified, corresponding to substages MIS 5e, 5c, and possibly 5a, based on sedimentological features, fossil assemblages, and Optically Stimulated Luminescence (OSL) dating. The oldest beach level (Sef-1) is attributed to MIS 5e (ca. 128–116 ka) and is characterised by the widespread presence of thermophilic Senegalese fauna—including *Thetystrombus latus*, *Conus ermineus*, and *Linatella caudata*—which mark the onset of this interglacial phase and are associated with two peaks in relative sea-level highstand. A subsequent cooling event during MIS 5d is recorded by the development of thin palaeosols and the disappearance of these warm-water taxa. The second beach level (Sef-2) reflects renewed sea-level rise and warmer conditions during MIS 5c, with abundant macrofauna and red algae. The transition to MIS 5b (~97 ka) is marked by a significant sea-level drop (down to –60 m), cooler climate, and enhanced colluvial sedimentation linked to increased runoff and erosion. In total, 54 macrofaunal species were identified—16 from Sef-1 and 46 from Sef-2—highlighting ecological shifts across substages. These results improve our understanding of coastal response to sea-level oscillations and paleoenvironmental dynamics in the western Mediterranean during the Late Pleistocene.

Keywords: sea-level changes; Marine Isotopic Stage 5; Late Pleistocene; Pityusic Island; Mediterranean thanatocoenoses

check for updates

Academic Editors: David Bridgland and Gemma Aiello

Received: 14 March 2025
Revised: 18 June 2025
Accepted: 2 July 2025
Published: 21 July 2025

Citation: del Valle, L.; Pons, G.X.; Fornós, J.J. Upper Pleistocene Marine Levels of the Es Copinar–Es Estufadors (Formentera, Balearic Islands, West Mediterranean). *Quaternary* **2025**, *8*, 38. https://doi.org/10.3390/quat8030038

Copyright: © 2025 by the authors. Licensee MDPI, Basel, Switzerland. This article is an open access article distributed under the terms and conditions of the Creative Commons Attribution (CC BY) license (https://creativecommons.org/licenses/by/4.0/).

1. Introduction

The Quaternary period is marked by alternating glacial phases with cold, arid conditions and interglacial phases characterised by warmer, more humid climates [1]. One of the most notable consequences of these climatic fluctuations is the global variation in sea levels, which has played a crucial role in shaping coastal geomorphology and influencing the habitats of numerous organisms. In this context, the transition from the penultimate glaciation (MIS 6) led to the onset of a warm interglacial phase, known as Marine Isotopic Stage (MIS) 5. This period facilitated the migration of intertropical marine mollusks, commonly referred to as Senegalese fauna, into the Mediterranean via the Strait of Gibraltar. However, as the interglacial substage MIS 5e (127–117 ka) came to an end, a widespread temperature decline occurred, gradually leading to the disappearance of these Senegalese species from the Mediterranean. Today, their distribution is limited to the West African

and Cabo Verde coasts [2]. The presence of these fauna is evident in the beach deposits along the Mediterranean coast, above the current sea level, and is considered of high stratigraphic value [3].

Multiple highstand sea-level events have been documented along the Mediterranean coasts, a region highly responsive to climatic fluctuations due in part to its semi-enclosed nature [4]. Climate and sea-level instability are evident in the faunal composition and the diverse facies present in its littoral deposits [5].

This study aims to analyse and interpret the climatic and sea-level variability of the Pleistocene in southeastern Formentera (Es Ram–Es Estufadors) by examining the sedimentological, compositional, and taxonomical characteristics of these littoral deposits. Additionally, it seeks to correlate these findings with the different climatic substages of MIS 5.

1.1. Geological and Physiographical Setting

Formentera is the smallest island of the Balearic Islands, with an area of 83.2 km^2, and belongs to the Pityusic Islands subgroup (Figure 1A). The island is characterised by relatively flat terrain, interrupted only by modest elevations such as Puig Guillen, located north of the Barbaria Cape, which rises to 107 m, and Pilar de la Mola the island's highest point at 202 m. The geology of Formentera is dominated by Quaternary and Upper Miocene deposits [6]. In particular, the island's substratum consists primarily of Miocene formations overlain by Quaternary deposits (Figure 1C). Two main fault systems, orientated 20° N-40° E and 120° N, influence the Upper Neogene and Pleistocene deposits (Figure 1C) [7]. These fault systems show evidence of Quaternary activity. Notably, recent tectonic activity has resulted in the deformation of sedimentary outcrops from the last interglacial to glacial period in the Es Copinar–Es Estufadors area [8].

The most representative marine sequences are found along the southeastern coast of Formentera, between Els Arenals and Punta de Ses Pesqueres (Figure 1C), covering approximately 0.7 km^2 of shoreline. The studied section lies along the island's southernmost coast, which stretches for about 3 km and includes four main sectors: Es Copinar, Caló des Mort, Es Ram, and Estufadors (Figure 1D). These successions rest atop a Miocene carbonate platform [9,10].

The Pleistocene marine fauna was first documented in the Es Copinar area [11]. Later research [12–14] identified Quaternary deposits and reported the occurrence of Senegalese fauna, including *Thetystrombus latus* (Formerly *Strombus bubonius*), in the same area.

The presence of Pleistocene marine fauna in Es Copinar and Es Ram was first reported by Gàsser and Ferrer [15], and later confirmed by Gàsser [10,16]. A detailed study of the sedimentary succession at Es Copinar and Caló des Mort emphasised its paleoclimatic significance and provided the first Optically Stimulated Luminescence (OSL) and palaeomagnetic dates [17]. Additional analyses of the Pleistocene sediments at Es Ram were carried out by Del Valle et al. [18]. These authors later extended their investigation to the deposits of Es Copinar, Caló des Mort, Es Ram, and Estufadors, incorporating OSL dating, chronostratigraphic fauna, and paleoclimatic reconstruction to interpret the coastal sequence from MIS 5e to MIS 2 [19]. In this context, the deposits overlying the Upper Miocene limestones correspond to Quaternary units [11–15,17,19–22]. These deposits consist, from bottom to top, of two well-defined marine levels, followed by a colluvial horizon, aeolianites that fossilise the underlying strata, interdunal palaeosols, dune and sand sheet formations, an additional colluvial layer, and, finally, units indicating aeolian–alluvial interaction [17–19].

In the Es Copinar–Es Estufadors section, six primary sedimentary facies and two palaeosols have been identified [19], categorised into three main associations, rep-

resenting colluvial–alluvial, marine, and aeolian sedimentary environments. This study focuses specifically on the marine deposits and associated units, with particular attention to the most recent marine level identified in the Es Estufadors area.

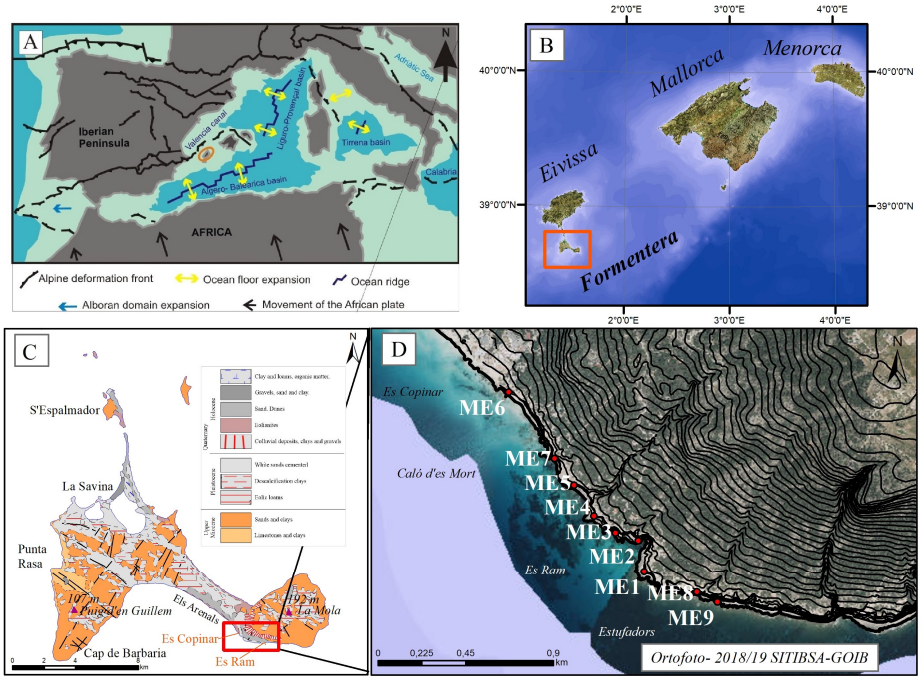


Figure 1. Study area location: (**A**) General tectonic framework (Modified from [23]); (**B**) Position of Formentera (red box) within the Balearic Archipelago [24]; (**C**) Geological map of Formentera, highlighting the study area (red box) (Modified from [25]); and (**D**) Topography and hydrology of the studied coastal section, indicating the location of the stratigraphic logs (Modified from [14]).

1.2. Mediterranean Water Circulation

The Mediterranean Sea, due to its semi-enclosed nature and east–west elongation, exhibits a predominantly anti-estuarine circulation pattern. This circulation is mainly driven by a negative water balance and a density gradient with the Atlantic Ocean [26–28]. Atlantic surface water, known as Modified Atlantic Water (MAW), enters the Alboran Sea through the Strait of Gibraltar (Figure 2) and occupies the upper 100–200 m of the water column. As it progresses eastward, MAW undergoes changes in salinity and temperature due to intense evaporation and regional mixing processes (Figure 3a) [28–30].

In the western basin, MAW forms a persistent anticyclonic gyre in the Alboran Sea before continuing along the North African coast as the Algerian Current, one of the key surface flows that redistribute water masses across the basin. Upon reaching the Sicily Channel, part of the MAW deflects northeastward, contributing to the Sicily Current, which influences the Tyrrhenian Sea and northern parts of the western basin, including the Balearic region. These regional currents play a crucial role in modulating sea-surface conditions, such as temperature and salinity, which in turn affect marine biogeography and paleoecological patterns.

In the Balearic Sea, circulation is also shaped by the Western Northern Current and the positioning of the North Balearic Front, a dynamic thermal boundary that separates the relatively warmer southern waters from the cooler northern flows. These features, along with dominant wind regimes, may have influenced past surface circulation patterns during interglacial stages and are thus relevant for interpreting paleoenvironmental records, particularly those linked to the distribution and retreat of thermophilic fauna like *Thetystrombus latus*.

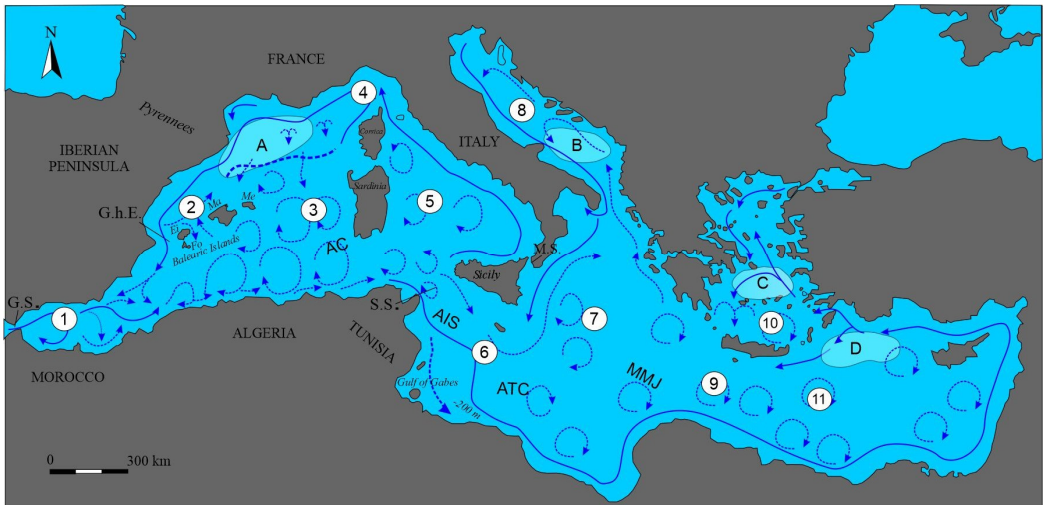


Figure 2. Scheme of modern circulation in Mediterranean (Modified from [27,28,31,32]). G.S.: Gibraltar Strait; M.S: Messina Strait, S.S: Sicily Strait; Ei: Eivissa; Fo: Formentera; Ma: Mallorca; Me: Menorca. Blue arrows indicate the following currents: AC (Algerian Current), AIS (Atlantic Ionian Stream), ATC (Atlantic Tunisian Current), and MMJ (Mid-Mediterranean Jet). Light blue dashed areas represent different deep-water masses: Mediterranean Deep Water (**A**), Eastern Mediterranean Deep Water (**B**,**C**), and Levantine Intermediate Water (**D**). White circles denote specific sea regions: (1) Alboran Sea, (2) Balearic Sea, (3) Alghero-Balearic Basin, (4) Ligurian Sea, (5) Tyrrhenian Sea, (6) Sicily Channel, (7) Ionian Sea, (8) Adriatic Sea, (9) Cretan Sea, (10) Aegean Sea, and (11) Levantine Sea.

1.3. Present Meteorological Conditions

The island has a typically Mediterranean climate, characterised by mild winters and warm summers, with limited rainfall, predominantly occurring in autumn and spring.

The annual average temperature is approximately 18 °C. The coldest month, January, has an average temperature of 11 °C, while the warmest month, August, averages around 26 °C. Precipitation is scarce and irregular, usually falling as torrential rain events, with an annual average of approximately 370 mm. During winter, prevailing winds include the Tramuntana (north), Mestral (northwest), and Gregal (northeast), all of which bring colder air masses. In contrast, summer is dominated by southerly winds such as the Migjorn, which carry warm air across the island.

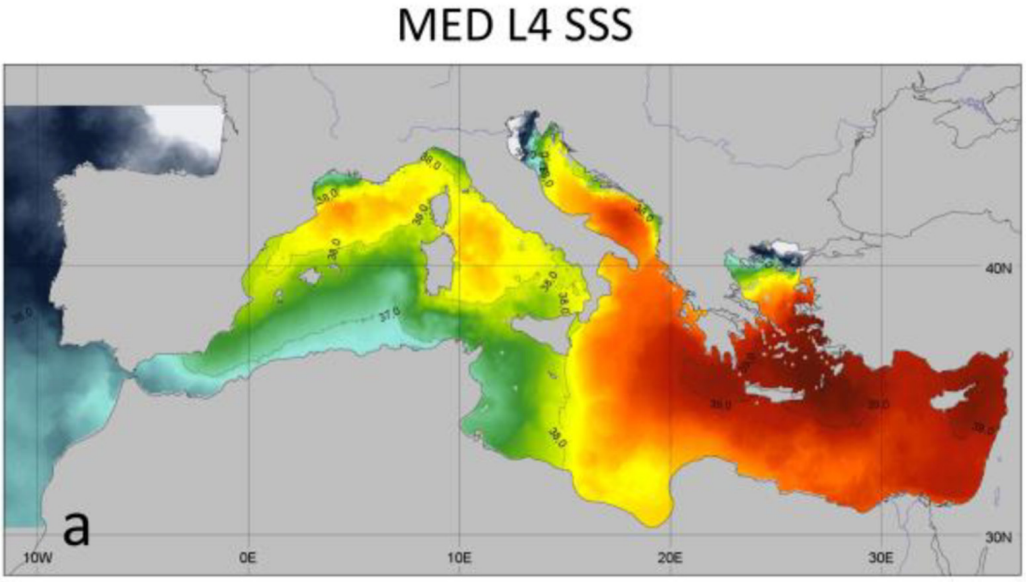


Figure 3. *Cont.*

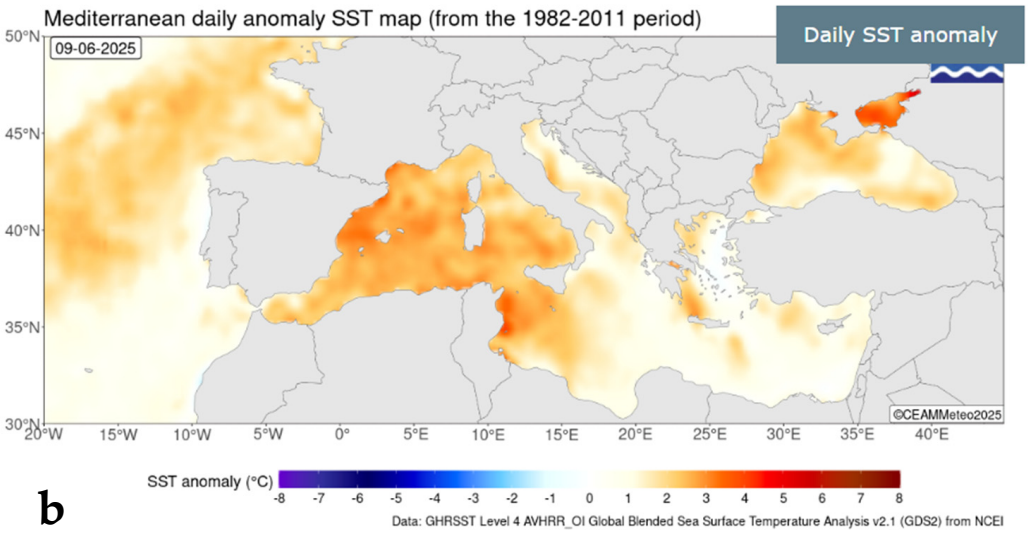


Figure 3. (**a**) Climatological sea surface salinity (SSS) in the Mediterranean Sea derived from the Copernicus Marine Service, showing the long-term average distribution of surface salinity based on the MEDSEA_REANALYSIS_PHY_006_004 product (1993–2022) [33]. (**b**) Daily sea surface temperature (SST) anomaly map for the Mediterranean on 9 June 2025, based on deviations from the 1982–2011 climatological mean, derived from the GHRSST Level 4 AVHRR_OI Global Blended SST Analysis (v2.1), provided by CEAM/Meteoce [34].

2. Materials and Methods

This study builds upon previous work by Del Valle et al. (2019, 2022) [18,19], which provided an initial stratigraphic framework and chronological interpretation of some Pleistocene deposits in the Es Copinar and Es Ram sectors. While those studies offered preliminary insights into the geomorphological evolution and climatic context of the coastal sequence, the present research incorporates new and more detailed stratigraphic data, including updated sedimentological descriptions, facies classification, and a comprehensive taxonomic inventory of marine macrofauna.

In particular, this paper presents, for the first time, systematic field analysis and detailed stratigraphic logging of the Es Estufadors sector, leading to the identification of a previously undocumented third marine level (Sef-3). Additionally, the quantitative analysis of grain composition, the application of the SedimPlak (ES2933384B2) counting method, and the correlation of stratigraphic profiles across the four main sectors (Es Copinar, Caló des Mort, Es Ram, and Es Estufadors) are original contributions of this study.

Stratigraphic sections were documented in the field and correlated based on the presence of prominent and extensive unconformities, homogeneous units, or continuous marine levels. Unconformities were identified as abrupt horizontal facies changes observed within the study area. Major units within each log were defined according to their mineralogical composition, grain size, and marine fauna content.

For marine fauna sample collection, a specific coding system was used depending on the sector: *Es Copinar* was labelled as EC, *Es Ram* as ER, and *Es Estufadors* as ES. All collected samples were catalogued with these codes and deposited in the Museum of the Societat d'Història Natural de les Balears.

Grain characteristic analysis was conducted using a binocular microscope equipped with MOTIC Image 2.0 software. Grain size analysis was performed using the open-source image analysis software IMAGE-J, combined with the point counting of 250 to 500 grains from each grain size fraction under a binocular microscope, employing the SedimPlak count and composition plate (ES2933384B2). Grains were classified into three categories: lithoclasts, bioclasts, and others.

Mineralogical content was determined using a Bruker D8-Advance X-ray diffractometer, with randomly oriented powder samples pre-treated with H_2O_2 to remove organic matter. Pressed powder diffraction patterns were recorded from 3° to 65° 2θ in 0.03° steps with a counting time of 0.3 s per step. The mineral phases were semi-quantitatively analysed using Diffrac EVA v.4.1 software, based on the integration of multiple diagnostic peaks, not solely the main peak. This approach allows for a more accurate estimation of relative mineral abundances—particularly for quartz—by accounting for peak area distribution and minimising potential errors caused by overlapping or background noise. The method applied follows standard semi-quantitative procedures widely used in sedimentological and mineralogical studies. The colour of sediments was described by Munsell Colour Chart [35]. For the taxonomic recognition of marine species, the World Register of Marine Species has been used [36] and validated morphological identifications through comparison with reference specimens from the Cuerda Collection housed at the Societat d'Història Natural de les Balears, which holds an extensive and regionally relevant assemblage of Quaternary marine mollusks.

Given the notable lateral and vertical variability observed within facies associations across different sectors of the study area, the results are presented by locality rather than by facies type alone. This site-based approach reflects differences in fossil assemblages, thickness, and sedimentary features, which are critical for interpreting depositional environments. Accordingly, within each sector, facies descriptions are followed by environmental interpretations.

3. Results

This section may be divided into subheadings and should provide a concise and precise description of the experimental results, their interpretation, and the derived conclusions.

3.1. Marine Facies

3.1.1. Sandy Beach

Description

In general, two beach levels can be identified and associated with different subenvironments, including the shoreface, backshore, and beachface.

The lower beach level (Sef-1) consists of highly cemented fine to medium bioclastic sand, showing a very pale brown colour (HUE 10YR 8/2- HUE 10YR 8/4). This level is characterised by a high abundance of disorganised marine fauna, including *Thetystrombus latus* (Figure 4A), *Conus ermineus*, and *Linatella caudata* (Figure 4B). Previous studies [10,14,16] have documented the presence of various marine species at this level, such as *Acanthocardia tuberculata*, *Amonia ephipphium*, *Arca noae*, *Glycymeris nummaria*, *Striarca lactea*, *Angulus* sp., *Cerithium vulgatum*, *Columbella rustica*, *Conus ventricosus*, *Conus ermineus*, *Linatella caudata*, *Chauvetia brunnea*, *Tritia cuvieri*, *Nassarius* sp., *Semicassis undulata*, *Crisilla semistriata*, *Thetystrombus latus*, *Stramonita haemastoma*, *Truncatella subcylindrica*, and *Hexaplex trunculus*. Our samples collected at this level (EC1, ER1, ER8, ES1 and ES4) show a greater biodiversity. In the Es Ram zone, we also identified *Lithophaga lithophaga*, *Mactra stultorum*, *Pseudochama gryphina*, *Venus verrucosa*, *Diodora gibberula*, *Patella caerulea*, *Rissoa* sp., and *Tricolia pullus*. In contrast, the Es Estufadors sector yielded *Bivetiella cancellata*, *Modiolus barbatus*, *Tritia cuvierii*, *Antalis vulgaris*, and several sea urchin spikes.

At Es Copinar, this unit overlies and fossilises the topographically irregular Upper Miocene basement, which exhibits a gentle slope toward the sea. Its maximum thickness reaches approximately 30 cm before it tapers off beneath the modern shoreline. This level is characterised by the ubiquitous presence of *Thetystrombus latus* (Figures 4A and 5A).

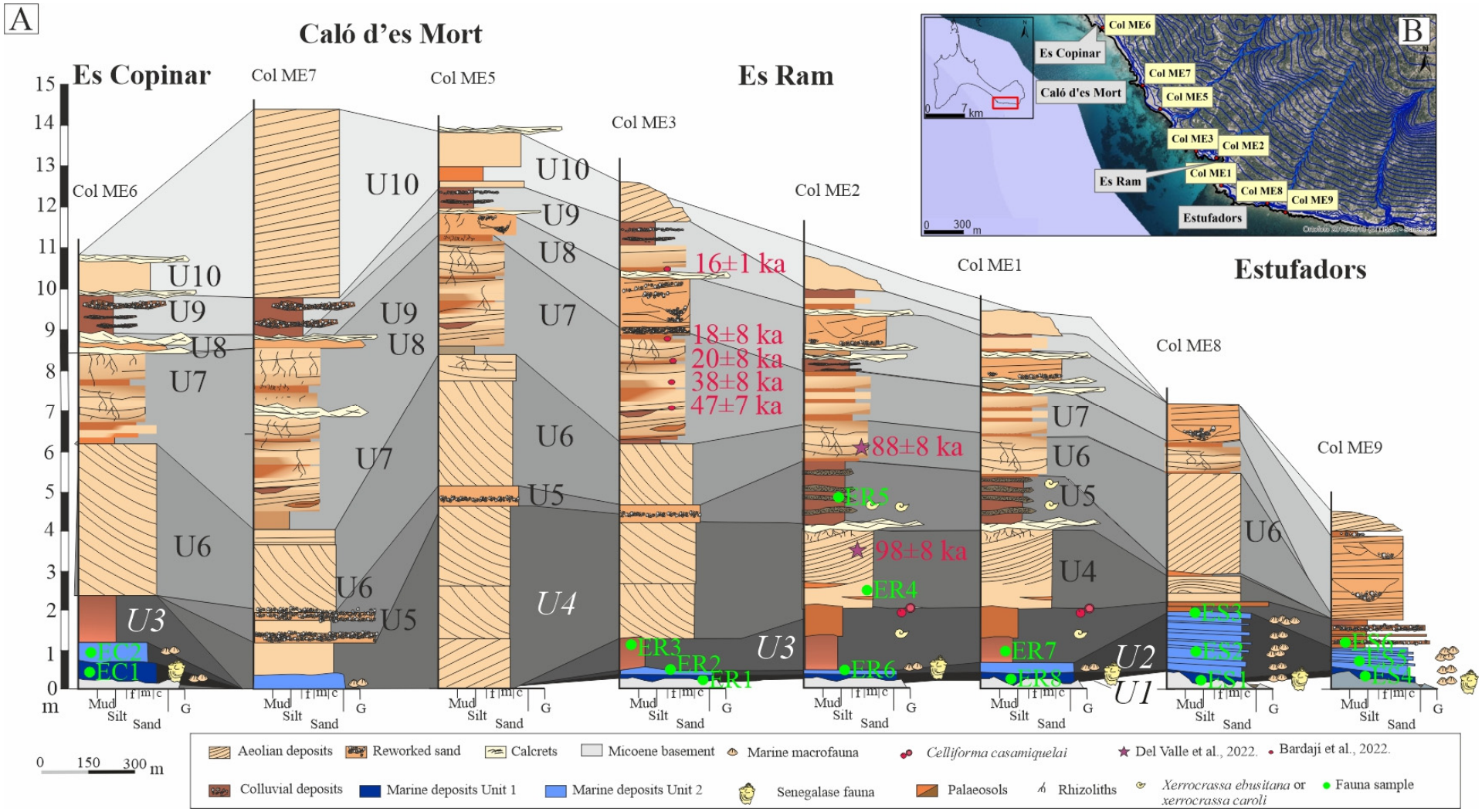


Figure 4. (**A**) Stratigraphic logs of the analysed outcrops, showing the distribution of sedimentary units and incorporating published OSL ages from Del Valle et al. [18,19]. Gray shading indicates the relative stratigraphic position of each unit, from the basal unit (U1) to the uppermost (U10). Green circles indicate the locations where faunal samples were collected. EC: Es Copinar; ER: Es Ram; ES: s'Estufadors. (**B**) Topographic map showing the precise locations of the stratigraphic logs referenced in (**A**).

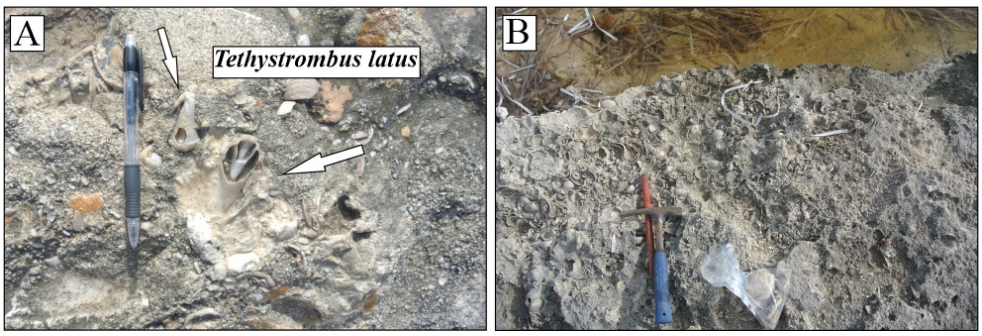


Figure 5. (**A**) Detail of the marine fauna species *Thetystrombus latus* present in the Es Copinar section (Lower beach level) Sef-1. (**B**) Marine fauna of the first beach level from Es Ram Sef-1.

In the areas of Es Ram and s'Estufadors, the unit is thinner—around 10 cm—and, in most cases, fills ancient basin depressions carved into the Miocene substrate (Figure 5B). Locally, a distinct layer composed of rounded and imbricated clasts, ranging in grain size from 2 to 6 cm, is observed from Es Ram to s'Estufadors.

Interpretation

The lower beach level (Sef-1) within this facies association is interpreted as the foreshore zone, influenced by high-energy wave activity and continuous sediment reworking. This interpretation is supported by the presence of well-sorted sand, ranging from fine to coarse grains, along with well-developed cross-bedding, features indicative of transport by waves and currents. The occurrence of Senegalese fauna (*Thetystrombus latus*, *Conus ermineus*, and *Linatella caudata*) suggests deposition under warm and humid environmental conditions. The overlying beach level (Sef-2) displays distinct sedimentological features characteristic of beach environments. It is composed of well-sorted, fine- to coarse-grained bioclastic sands, exhibiting a white to very pale brown colouration (HUE 10 YR 8/1–HUE 10 YR 8/2). This unit contains sub-horizontal to low-angle (approximately 5°) seaward-dipping lamination (Figure 6A), forming inclined bedding relative to the underlying surface.

Additionally, Sef-2 is structured into alternating horizons: some enriched with well-organised layers of marine fauna, 1 to 3 cm thick (Figure 5B), and others consisting of sandy laminae, 1 to 2 cm in thickness (Figure 6C). The marine fauna identified within this level include *Acanthocardia tuberculata*, *Amonia ephipphium*, *Chamelea gallina*, *Glycymeris nummaria*, *Lima lima*, *Bolma rugosa*, *Nassarius* sp., *Semicassis undulata*, *Stramonita hemastoma*, *Trochidae*, *Lithothamium* sp., and sea urchin spines (Figure 6C) [16].

In the levels with abundant marine macrofauna, the matrix is significantly finer, and the proportion of bioclasts relative to lithoclasts is 98.85%, corresponding predominantly to a rudstone texture. In contrast, areas with a lower presence of marine macrofauna—characterised by a floastsone texture—exhibit slightly coarser grain sizes, consisting mainly of medium sands ranging from 500 to 1000 μm. These samples still show a high bioclast content, with an average of 97.5% in each level studied, based on counts of 500 grains per sample.

Variations in faunal composition are observed across different sites. At Es Copinar, there is a clear dominance of two lamellibranch species: *Glycymeris nummaria* and *Chamelea gallina* (Figure 7A,B).

Several new faunal elements have been identified, complementing those previously described by [16] in the levels (Sef-2)—(ER2, ER3 ER6). These include *Barbatia barbata*, *Clausinella fasciata*, *Varicorbula gibba*, *Ctena decussata*, *Chama gryphoides*, *Loripes orbiculatus*, *Ostrea stentina*, *Polititapes aureus*, *Bittium reticulatum*, *Cerithium lividulum*, *Gibberula miliaria*, *Tritia cuvierii*, *Pusia ebenus*, and *Antalis vulgaris*.

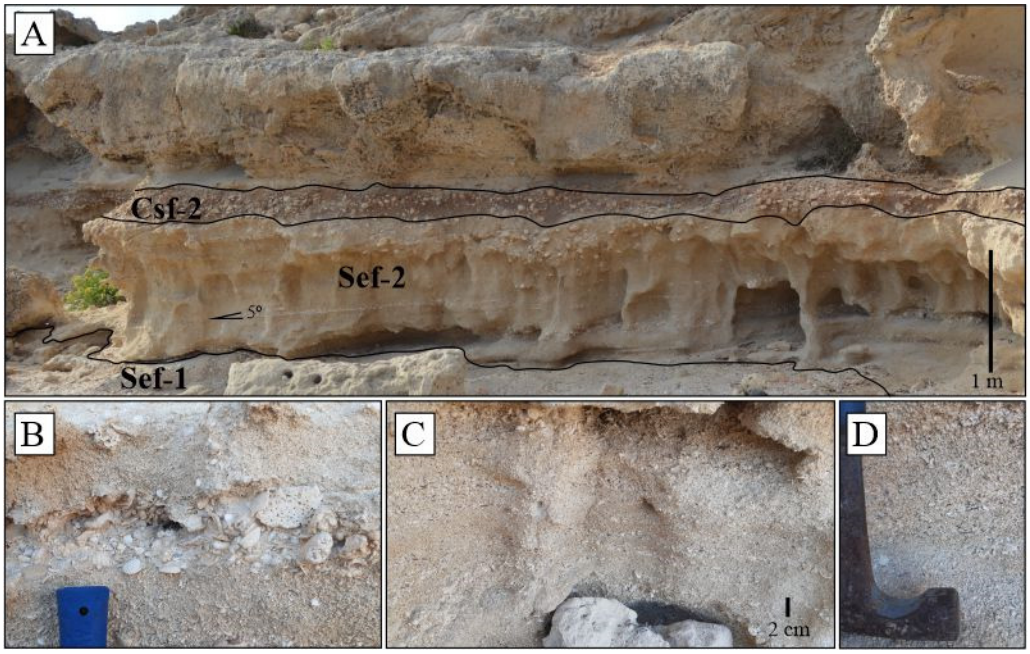


Figure 6. (**A**) General view of the Late Pleistocene deposits in the Es Estufadors area. (**B**) Detail of the second marine level (Sef-2), showing its internal structure and contact with overlying aeolian units. (**C**,**D**) Stratification of Sef-2, characterised by alternating fossil-rich and sandy laminae. These deposits rest unconformably above the colluvial facies Csf-2, which appears as a reddish silty-breccia at the base of the section. The underlying Csf-1 facies is not exposed in this outcrop, as it is very thin and located beneath the marine units, often masked by the irregular Miocene basement.

ER3: *Callista chione*, *Tritia pellucida*, *Diodora gibberula*, *Gibbula divaricata*, *Gibbula* sp., *Tricolia pullus*, *Scaphopoda*, *Poliplacophora*.

ER6: *Laevocardium oblongum*, *Pecten jacobeus*, *Spondylus gaederopus*, *Venus verrucosa*, *Euthria cornea*, *Ocenebra erinaceus*, *Phorcus turbinatus*, *Patella ulyssiponensis*, *Rissoa decorata*, *Stramonita haemastoma*, *Monophorus perversus*, *Turritellinella tricarinata*, *Vermetus triquetrus*, and sea urchin spines.

In the Es Estufadors sector, the middle beach level (Sef-2) is well-exposed and is characterised by a predominance of bivalve species, including *Chamelea gallina*, *Glycymeris bimaculate*, and *Glycymeris nummaria*. In the lower portion of this level, lenses of red algae, approximately 10 cm thick, are also present. These are followed by a sequence of sandy layers (ES2, ES5), which contain a high abundance of echinoid spines (Figure 7D), as well as fauna-rich levels dominated by fragmented shells within a sandy matrix—displaying a floastone texture—and the presence of completed adult specimens of *Pecten jacobeus* (approximately 10–12 cm diameter) (Figure 8A).

In the central portion of this level, the following species have been identified: *Acanthocardia tuberculata*, *Arca noae*, *Chamelea gallina*, *Glycymeris nummaria*, *Pecten jacobeus*, *Bittium reticulatum*, *Rissoa* sp., *Monophorus perversus*, *Poliplacophora*, and *Lithothamium* sp. Approximately 10 cm below the top of the Sef-2 in Es Estufadors, a concentration of marine macrofauna was found within layer ES5. Additional species identified in this horizon include *Chama gryphoides*, *Glycymeris nummaria*, *Lima lima*, *Loripes orbiculatus*, *Spondylus gaederopus*, *Bolma rugosa*, *Conus ventricosus*, *Steromphala divaricata*, *Trochidae*, *Vermetus triquetrus*, *Scaphopoda—Antalis vulgaris* (Figure 8B,C).

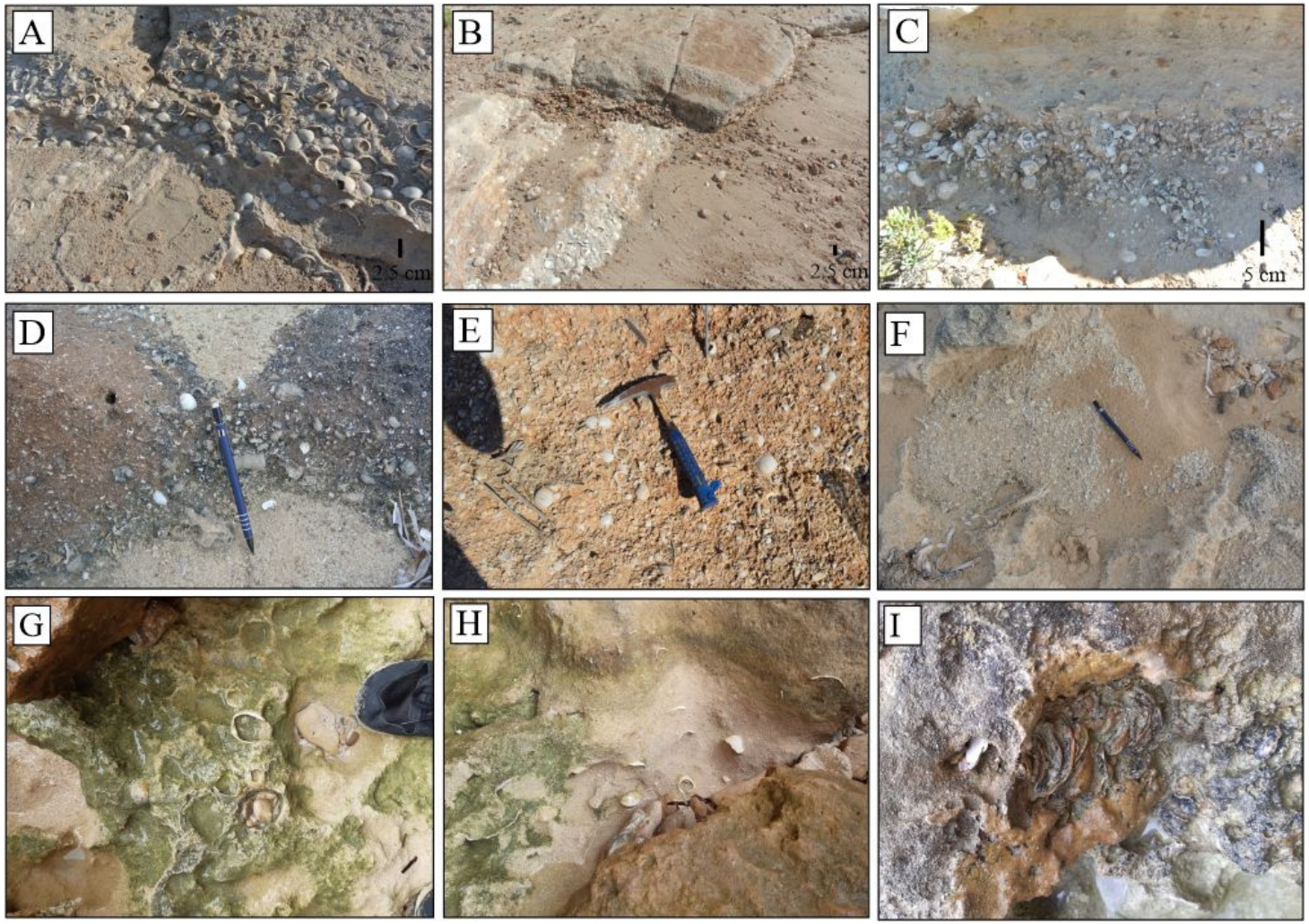


Figure 7. (**A**,**B**) General view or aspect of the second marine level characterised by the abundant presence of *Glycymeris nummaria* and *Chamelea gallina* in Es Copinar, Sef-2. (**C**–**F**) Abundant marine fauna is present in the second level of Es Ram, Sef-2. (**G**,**H**) Detailed views of the Sef-2 level at Caló des Mort, a newly identified exposure described here for the first time by the authors. The images show the sedimentary structure and stratification of this upper beach unit, Sef-1. (**I**) Close-up image of a karstic cavity (cocoons) filled with marine deposits, notably lacking Senegalese fauna, suggesting a distinct depositional or post-depositional environment compared to nearby fossil-rich levels, Sef-3.

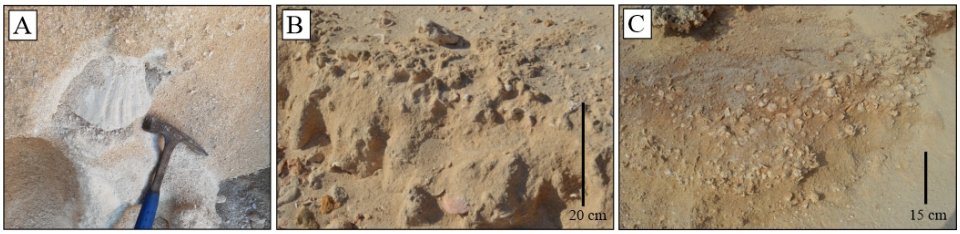


Figure 8. (**A**) *Pecten jacobeus* in Es Estufadors area, second marine level Sef-2. (**B**,**C**) Different horizons of the second marine level present in Es Estufadors Sef-2.

The second beach level (Sef-2) is interpreted as a wave-dominated, microtidal sandy beach system, extending from the submerged to the subaerial zone. The presence of well-preserved, mostly adult shells with minimal fragmentation, embedded within a sand-rich matrix and accompanied by a high abundance of two dominant marine species (*Glycymeris nummaria* and *Chamelea gallina*), suggests deposition in a relatively low-energy, calm water environment.

Comparable sedimentary deposits have been reported at several sites across the Western Mediterranean basin [37], including Sardinia and Mallorca, where similar stratigraphic levels have been documented [38,39].

Currently, in the Es Copinar area, part of the fossil beach is overlain by a dense accumulation of bivalves (mainly *Glycymeris* sp.), highlighting the biological productivity of the area. This observation supports the interpretation that similar environmental conditions—warm and humid, characteristic of an interglacial period—have recurred at this site in the past (Figure 9).



Figure 9. (**A**,**B**) Basin-shaped depressions carved into the Miocene basement infilled with modern marine sediments, rounded clasts, and anthropogenic materials, observed at Es Estufadors Sef-3. (**C**) Present-day beach level at Es Copinar, displaying a dense accumulation of marine fauna, including numerous echinoid spines.

3.2. Colluvial Facies Association

3.2.1. Silty-Breccia with Marine Shells and Palaeosols

Description

According to [19], this facies association (Csf) consists of very poorly to poorly sorted breccia with a silty matrix containing floating granules. The texture is matrix-supported, with angular clasts ranging from pebble to boulder size, primarily composed of angular limestone fragments derived from the Miocene basement. Interbedded within the breccia levels are palaeosol horizons containing floating clasts (Figure 10A).

The palaeosols are composed of reddish-brown (HUE 5YR 6/8) silty to muddy sediments with a massive structure. They range in thickness from 15 to 50 cm and contain scattered, lens-shaped clast lags up to 30 cm thick. The lower part of the colluvial deposit is marked by an erosive basal contact and a high concentration of marine shell fragments (Figure 10B,C). Marine fauna identified in sample ES6 include *Arca noae*, *Chama gryphoides*, *Chamelea gallina*, *Lima lima*, *Spondylus gaederopus*, *Bolma rugosa*, *Vermetus triquetrus*, *Lithothamnium* sp., and abundant red algae (Figure 10B–D). The total thickness of the deposit ranges from 25 to 45 cm.

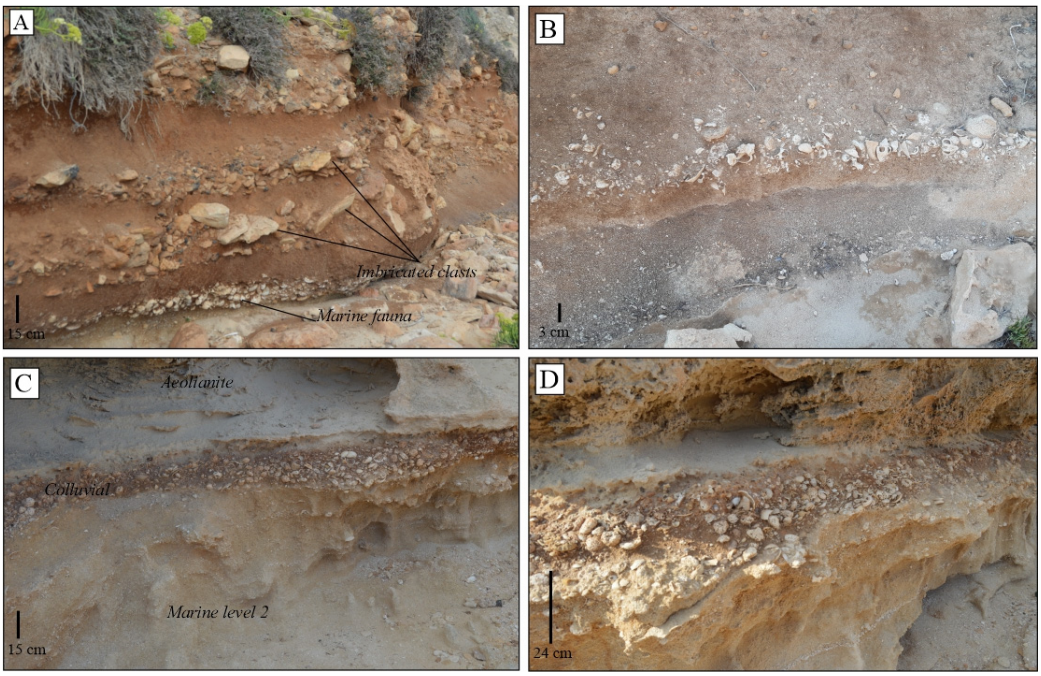


Figure 10. (**A**–**D**) Es Estufadors Pleistocene deposits, facies composed of silty colluvium with marine shells and palaeosols Csf 2.

X-ray diffraction analysis revealed a significant quartz content (35%), in contrast to the aeolian levels, where quartz percentages range between 1% and 5%.

Interpretation

These deposits are interpreted as colluvial sediments formed by a combination of sheet flow and debris-flow processes. The presence of palaeosols indicates phases of sedimentary stabilisation and intense weathering [40–42]. Lateral variations in bed geometry appear to be controlled by the irregular topography of the underlying Miocene basement.

According to Rodríguez-López et al. (2012) [43], the presence of deflation lags and palaeosols overlying these water-laid deposits suggests that water discharge events were episodic, separated by intervals of aeolian deflation. Furthermore, the presence of reworked marine fauna—including *Stramonita haemastoma*, *Pecten jacobeus*, *Bolma rugosa*, *Arca noae*, and *Glycymeris* sp.—indicates that occasional reworking processes incorporated material from underlying marine units into the colluvial deposits.

4. Discussion

OSL dating results from the aeolian units overlying the marine sequences, as reported by [19], yield ages of 98 ± 8 ka and 88 ± 8 ka (Figure 11). In addition, biochronostratigraphic data from both marine and colluvial deposits containing marine fauna indicate deposition during Marine Isotopic Stage (MIS) 5. More specifically, the lower beach level is attributed to the substage MIS 5e, while the overlying level corresponds stratigraphically to MIS 5c. However, an assignment to MIS 5a cannot be entirely ruled out, considering the associated dating uncertainties. Recent studies on nearby Mallorca [44] suggest that, during MIS 5a, sea level stood approximately one meter above the present mean sea level.

The environmental evolution of the Es Copinar–Estufadors coastal system began during the onset of MIS 5e (~127 ka) (Figure 12A). This period was marked by a summer temperature anomaly of approximately +2 °C in mid- and low-latitude regions [44]. Sea level during this time varied regionally and globally, ranging from + 3 m to + 9 m above present sea level, representing the first major highstand of the Late Pleistocene. This

transgression is recorded in sediments containing warm-water fauna, including *Thetystrombus latus* (e.g., *Strombus bubonius*), *Linatella caudata* (e.g., *Cantharus viverratus*), and *Conus ermineus* (e.g., *Conus testudinarius*).

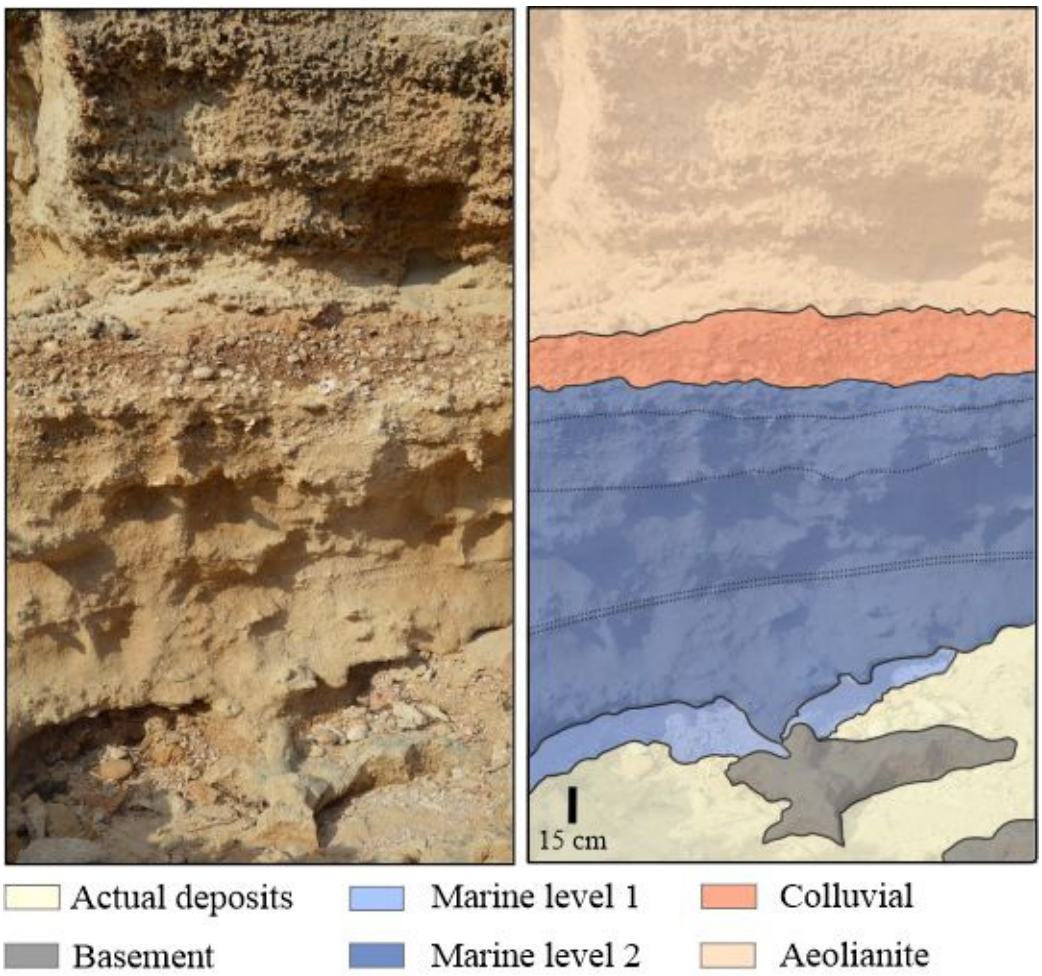


Figure 11. Sketch of the different levels identified in Es Estufadors area. Marine level 1 Sef-1, Marine level 2 Sef-2, Colluvial Csf 2, Aeolinate Sel-1.

Widespread evidence of MIS 5e sea-level highstands has been documented across the Mediterranean (Figure 13), including in Mallorca [14,38], Italy [45], Sardinia [39,46,47], Liguria [48], Calabria [49], Tuscany [50], southern Spain [27,51], Morocco [52,53], Tunisia [51,54], and Israel [51,55]. A defining feature of these deposits is the presence of the thermophilic "Senegalese" faunal assemblage. Globally, equivalent beach deposits from MIS 5e have also been reported in South Africa [56,57], the Bahamas [58,59], and Australia [60]. The modern distribution of this fauna, restricted to the coasts of West Africa and Cape Verde, suggests that it thrives in waters with annual sea surface temperatures of ~23–24 °C and winter minima not below 19–21 °C, within a salinity range of 34–35‰ [2,27,61]. Its past distribution in the Mediterranean is thought to have been favoured by the influx of fresher Atlantic waters (Modified Atlantic Water, MAW) (Figure 2).

During MIS 5d, a shift to cooler, more arid conditions occurred, resulting in the development of thin palaeosols. These correlate with pedogenetic horizons identified in the study area. This climatic deterioration likely led to the cooling of Mediterranean waters, contributing to the regional extinction of Senegalese species, particularly *Thetystrombus latus*.

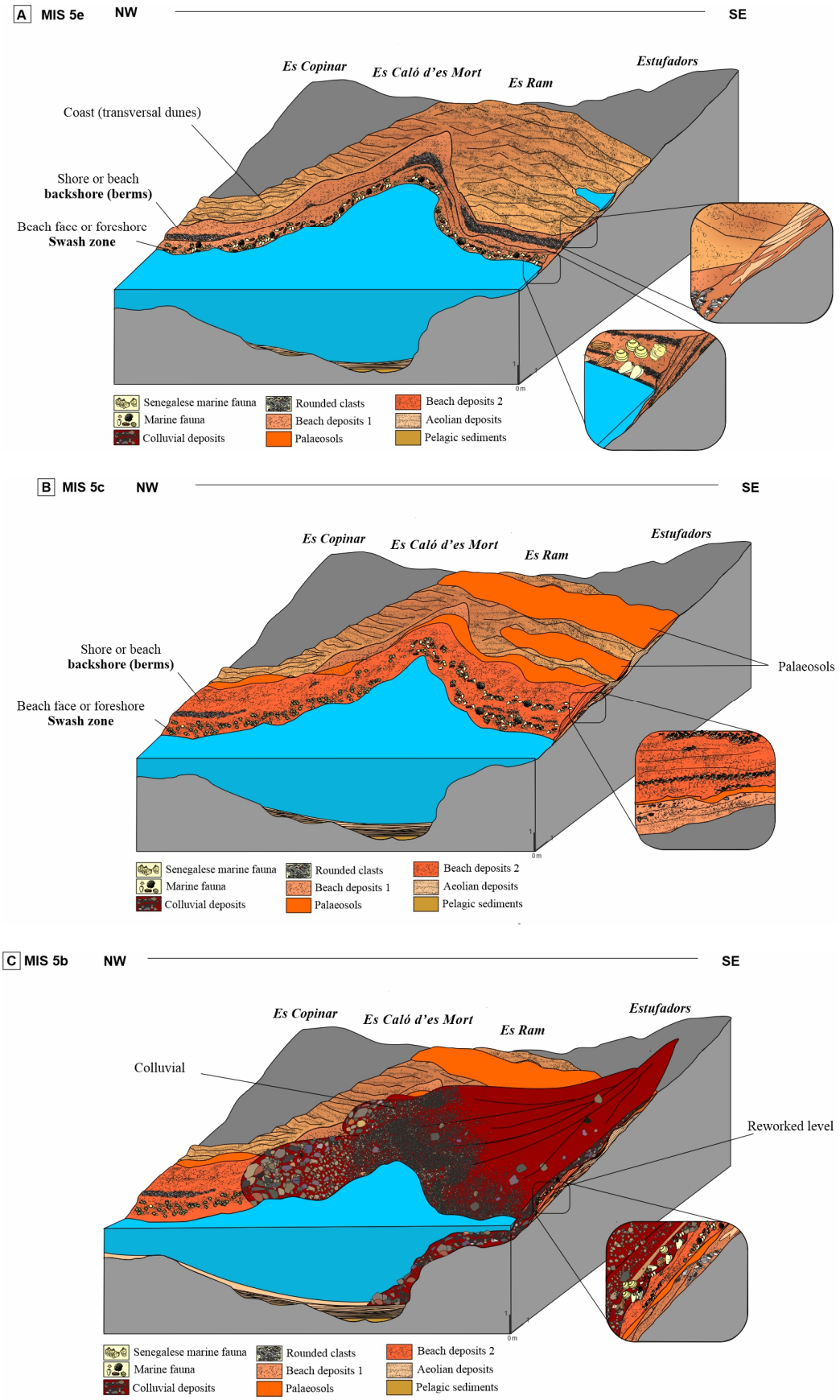


Figure 12. Geomorphological evolution model of Es Copinar to Es Estufadors area. (**A**) Interglacial substage MIS 5e. (**B**) interglacial MIS 5c and (**C**) cooler substage MIS 5b.

MIS 5c marked a sea-level rise and a relatively warm interval [62–64], which supported the formation of a new beach system rich in marine macrofauna, including *Glycymeris nummaria*, *Arca noae*, *Patella caerulea*, and *Conus ventricosus* (Figure 12B, Unit U2). Multiple highstands from MIS 5c have been identified along the Spanish coastline and other Mediterranean locations, including Cala en Baster (Formentera's northern coast) [37], NW Liguria [65], Italy [65]; Tuscany [50]; Sardinia [39,46,66]; Alghero, Tunisia [67]; the Carmel coast in Israel [68]; and Alexandria, Egypt [69].

Similar multilevel marine terraces correlated with MIS 5 substages have also been documented in other Mediterranean contexts, notably along the Cilento Promontory (Italy), where [70] described stepped terraces and associated faunal assemblages that match the timing and ecological signals of MIS 5e to 5a. Their correlation highlights a synchronous regional sea-level response and emphasises the broader Mediterranean signature of these transgressive-regressive cycles.

Furthermore, the morpho-sedimentary and ecological analyses carried out by [71] in the Western Mediterranean provide a valuable framework to interpret marine deposits in Formentera. Their work, which integrates bathymetric and stratigraphic data, demonstrates that MIS stages can be clearly differentiated based on seafloor morphology and sedimentary facies, supporting the interpretation of the studied levels as highstand beach deposits corresponding to MIS 5e and 5c. These correlations enhance the robustness of regional comparisons and reinforce the paleoclimatic significance of the deposits analysed in this study.

The cooling event during MIS 5c/b transition (~97 ka) triggered a significant sea-level drop, with values reaching between –16 and –60 m [72–75]. This decline was linked to increasing aridity and a sharp decrease in average sea surface temperatures—from ~18 °C during MIS 5c to ~10 °C during MIS 5b [76,77].

In the Balearic Islands, average temperatures decreased by nearly 10 °C, reaching ~6.7 °C during the MIS 5b [38,78].

These environmental changes—marked by a transition to cooler and more arid conditions during the MIS 5c to MIS 5b interval—likely resulted in a significant reduction in vegetation cover. This interpretation is supported by the absence of typical pedogenic features usually associated with vegetated soils in the western Mediterranean, such as rhizoconcretions, root casts, or bioturbation structures. The colluvial deposits are composed of poorly sorted breccias with angular clasts, suggesting intense surface runoff and slope instability, which are consistent with low or absent vegetative protection. Additionally, the palaeosol horizons observed are weakly developed, with massive reddish-brown silty textures (Munsell 5YR 6/8) and lack clear evidence of rooting or pedogenic horizonation. Together with the broader regional paleoclimatic evidence for increased aridity and temperature decline during this period, these features support the interpretation of a landscape with minimal vegetation cover, promoting erosion and intermittent soil development (Figure 12C).

In general terms, the present study shows clear evidence of sea-level fluctuations, which occurred during the late Pleistocene associated to climatic changes, which resulted in the extinction of thermophilic fauna, *Thetystrombus latus*, *Conus testudinarius*, and *Linatella caudata*.

It is also notable that fifty-four faunal species have been newly identified in the study area—sixteen from the first beach level and forty-six from the second. A significant finding is the faunal overlap between the second beach level (Sef-2) and the colluvial facies, confirming that the marine fauna found in the reworked colluvial levels originated from underlying marine deposits.

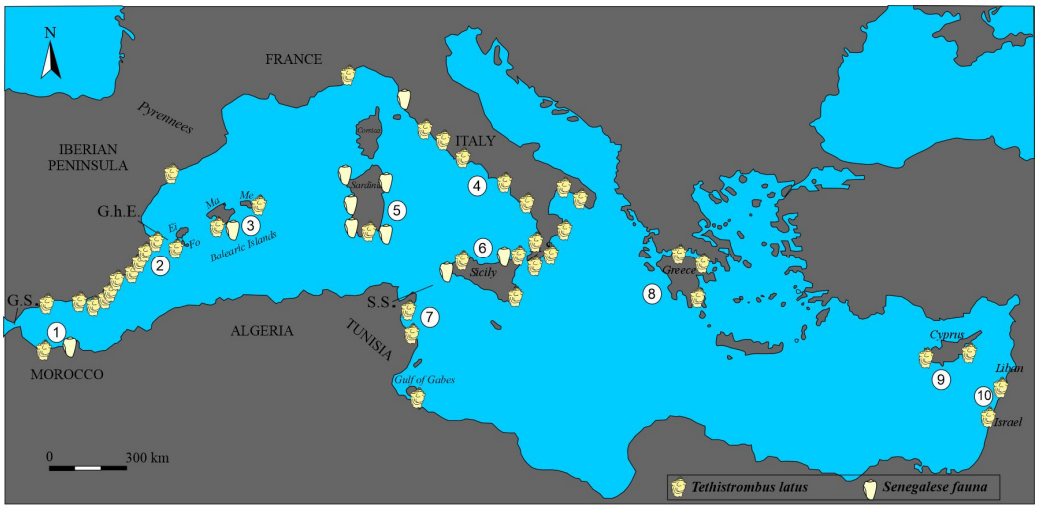


Figure 13. Scheme of *Tethystrombus latus* and Senegalese fauna fossil location in the Mediterranean, from 1—Morocco [52,53], 2—Iberian Peninsula (South Spain [5,27,51,79]), 3—Balearic Islands, Formentera [16,17,19], Mallorca [3,14,38], Menorca (Cala Galdana [80]; 4—Italy [27,45], Taranto [81]; 5—Sardinia [39,46,47,66,82,83]; Tuscany [45,50]; Rome [84], 6—Sicily [61]; 8—Greece [85–87], 9—Cyprus [61,88]; 10—Libya [61,89]; Israel [55,90], 7—Tunisia [51,54,90]; Carmel [91]; Liguria [48]; Calabria [49].

5. Conclusions

In the Es Copinar–Es Estufadors area, fifty-four new records of marine macrofauna species have been identified within the Late Pleistocene deposits. These include sixteen species associated with the first beach level and forty-six species linked to the second, confirming the presence of the chronostratigraphically significant Senegalese fauna in the region.

Three beach levels corresponding to MIS 5 (Sef-1, Sef-2, and Sef-3) have been documented in the Es Estufadors for the first time. Based on Optically Stimulated Luminescence (OSL) dating and the presence of a diagnostic biochronostratigraphic species such as *Thetystrombus latus*; *Linatella caudata*, and *Conus ermineus*, it is concluded that the first beach level (Sef-1) was deposited during MIS 5e (~127 ka), a period when the sea level reached approximately + 3 m above present mean sea level across the Mediterranean.

The climatic deterioration during MIS 5d resulted in a marked drop in temperature, leading to the cooling of Mediterranean waters and the local extinction of Senegalese fauna—notably *Thetystrombus latus*.

During Marine isotopic Stage (MIS) 5c and possibly MIS 5a, a sea-level rise occurred during a relatively warm phase, facilitating the formation of a second beach system rich in marine macrofauna, including *Glycymeris nummaria*, *Arca noae*, *Patella caerulea*, *Conus ventricosus*, and associated red algae.

During the Marine Isotopic Stage MIS 5c/5b transition (~97 ka), sea level fell to below –60 m, signalling the onset of more arid conditions. This environmental shift led to episodic but intense rainfall events and increased slope runoff, which, coupled with a lowered base level and reduced vegetation cover, promoted widespread soil erosion. These processes ultimately contributed to the reworking and incorporation of second beach level materials into overlying colluvial deposits.

Overall, these findings provide valuable insight into the geomorphological dynamics and climatic fluctuations of the Late Pleistocene, contributing to a deeper understanding of the Pleistocene evolution of the western Mediterranean region.

Author Contributions: L.d.V. conceptualised and designed the analysis, collected the data, contributed data and analytical tools, conducted the analysis, and drafted the manuscript. G.X.P. classified the fossil marine fauna, contributed analytical tools, and revised the text. J.J.F. provided data and reviewed the manuscript. All authors have read and agreed to the published version of the manuscript.

Funding: This research was supported by the Agencia Estatal de Investigación (AEI) under grant number PID2020-112720GB-I00/AEI/10.13039/501100011033 and Chronic Emergencies and Ecosocial Transformations in Touristified Coastal Spaces PID2022-137648OB-C21. Funding was provided by MCIN/AEI/10.13039/501100011033 and co-financed by "ERDF A way of making Europe".

Data Availability Statement: Data available on request from the authors.

Acknowledgments: We would like to thank the Societat d'Història Natural de les Balears (SHNB) for granting access to the Cuerda Collection, which was essential for the taxonomic validation of marine fauna. We are also grateful to Miguel McMinn for his careful review and correction of the English throughout the manuscript. His contributions significantly improved the clarity and fluency of the text.

Conflicts of Interest: The authors declare no known financial or personal conflicts of interest that could have influenced the research presented in this paper.

References

1. Murray-Wallace, C.V.; Woodroffe, C.D. The causes of Quaternary sea-level changes. In *Quaternary Sea-Level Changes: A Global Perspective*; Cambridge University Press: Cambridge, UK, 2014; pp. 41–78.
2. Zazo, C.; Goy, J.L.; Hillaire-Marcel, C.; Dabrio, C.J.; González-Delgado, J.A.; Cabero, A.; Bardají, T.; Ghaleb, B.; Soler, V. Sea level changes during the last and present interglacials in Sal Island (Cape Verde archipelago). *Glob. Planet. Change* **2010**, *72*, 302–317. [CrossRef]
3. Vicens, D. El Registre Paleontològic Dels Dipòsits Litorals Quaternaris a l'illa de Mallorca (Illes Balears, Mediterrània Occidental). Ph.D. Thesis, University of the Balearic Islands, Palma, Spain, 2015; p. 1011.
4. Martínez-Ruiz, F.; Kastner, M.; Gallego-Torres, D.; Rodrigo-Gámiz, M.; Nieto-Moreno, V.; Ortega-Huertas, M. Paleoclimate and paleoceonography over the past 20,000 yr in the Mediterranean Sea Basins as indicated by sediment elemental proxies. *Quat. Sci. Rev.* **2015**, *107*, 25–46. [CrossRef]
5. Zazo, C.; Goy, J.L.; Dabrio, C.J.; Lario, J.; González-Delgado, J.A.; Bardají, T.; Hillaire-Marcel, C.; Cabero, A.; Ghaleb, B.; Borja, F.; et al. Retracing the Quaternary history of sea-level changes in the Spanish Mediterranean-Atlantic coasts: Geomorphological and sedimentological approach. *Geomorphology* **2013**, *196*, 36–49. [CrossRef]
6. Costa, M.; Cuerda, J.; Rosselló, V.M. Formentera i els estanys. Panorama geològic des del Quaternari. *Cuad. Geogr.* **1985**, *37*, 75–96.
7. Somoza, L.; Medialdea, T.; Terrinha, P.; Ramos, A.; Vázquez, J.T. Submarine Active Faults and Morpho-Tectonics Around the Iberian Margins: Seismic and Tsunamis Hazards. *Front. Earth Sci.* **2021**, *9*, 653639. [CrossRef]
8. Bardají, T.; Roquero, E.; Cabero, A.; Zazo, C.; Goy, J.L.; Dabrio, C.J.; Machado, M.J.; Lario, J.; Silva, P.G.; Martínez-Graña, A.M. Abrupt environmental changes during the last glacial cycle in Western Mediterranean (Formentera Island, Balearic archipelago). *Quat. Int.* **2022**, *638–639*, 159–179. [CrossRef]
9. Gàsser, Z. Descripció del jaciment del Miocè marí a s'estufador (Formentera, Illes Pitiüses, Mediterrània occidental). *Boll. Soc. Hist. Nat. Balears* **2001**, *44*, 87–92.
10. Gàsser, Z. Jaciments paleontològics marins del Miocè i Quaternari d'es Ram (Formentera, Illes Pitiüses). *Boll. Soc. Hist. Nat. Balears* **2002**, *45*, 87–92.
11. Butzer, K.W.; Cuerda, J. Coastal stratigraphy of southern Mallorca and its implication for the Pleistocene chronology of the Mediterranean Sea. *J. Geol.* **1962**, *70*, 398–416. [CrossRef]
12. Cuerda, J. A Contribution to the Knowledge of Pleistocene Coastal Profiles. In *Biogeography and Ecology of the Pityusic Islands*; Kuhbier, H., Alcover, J.A., Guerau d'Arellano, C., Eds.; Monographiae Biologicae; Springer: The Hague, The Netherlands, 1984; Volume 52, pp. 105–118.
13. Cuerda, J. *Moluscos Marinos y Salobres Del Pleistoceno Balear*; La Caja de Baleares "Sa Nostra": Palma, Spain, 1987; p. 421.
14. Cuerda, J. *Los Tiempos Cuaternarios en Baleares*, 2nd ed.; Conselleria de Cultura, Educació i Esports del Govern Balear: Palma, Spain, 1989; p. 305.

15. Gàsser, Z.; Ferrer, J.A. Nous jaciments paleontològics del Miocè i Quaternari de Formentera (Illes Pitiüses, Mediterrània Occidental). In *Bolletí de la Societat d'Història Natural de les Balears*; Societat d'Història Natural de les Balears: Palma de Mallorca, Spain, 1997; Volume 40, pp. 91–101. ISSN 212-260X.
16. Gàsser, Z. Nota paleontològica sobre el jaciment quaternari marí d'Es Copinar (Formentera, Illes Pitiüses, Mediterrània occidental). *Boll. Soc. Hist. Nat. Balears* **1998**, *41*, 153–157.
17. Bardají, T.; Cabrero, A.; Roquero, E.; Zazo, C.; Lario, J.; Dabrio, C.J.; Goy, J.L.; Machado, M.J.; Mercier, N.; Silva, P.G.; et al. Climatic variability in western Mediterranean during the last glacial cycle (ca. 130–114 ky BP): Evidences from an island setting (Formentera, Balearic Is., Spain). In Proceedings of the PAGES 5th Open Science Meeting, Zaragoza, Spain, 9–13 May 2017.
18. Del Valle, L.; Timar-Gabor, A.; Fornós, J.J. Late Pleistocene Coastal Deposits of South-Western Formentera (Western Mediterranean): Chronology, Landscape Evolution and Climatic Variability. In Proceedings of the IAS Conference, Rome, Italy, 10–13 September 2019.
19. Del Valle, L.; Timar-Gabor, A.; Pomar, F.; Pons, G.X.; Fornós, J.J. Millennial-scale climatic variability recorded in Late Pleistocene coastal deposits of Formentera Island (Balearic Archipelago, Western Mediterranean). *Quat. Int.* **2022**, *617*, 112–128. [CrossRef]
20. Solé Sabarís, L. Le quaternaire marin des Baléares et ses rapports avec les côtes méditerranéennes de la Péninsule Ibérique. *Quaternaria* **1962**, *6*, 309–342.
21. Parenzano, P. *Carta D'Identitá Delle Conchiglie Del Mediterraneo. Volume Primo*; Gasteropodi, Bios Taras Editrice: Taranto, Italy, 1970.
22. Díaz, J.A. Guía de la Geología de Granada, 2009. Available online: http://www.granadanatural.com/blog.php?codigo_blog_articulo=63 (accessed on 2 September 2021).
23. Vicens, D.; Gràcia, F.; Cuerda, J. El Quaternari marí del torrent Fondo (Formentera, Illes Pitiüses). *Boll. Soc. Hist. Nat. Balears* **1992**, *35*, 61–66.
24. SITIBSA. Available online: https://ideib.caib.es/visor/ (accessed on 26 January 2025).
25. IGME. Available online: https://info.igme.es/cartografiadigital/geologica/Magna50Hoja.aspx?Id=798&language=es (accessed on 26 January 2022).
26. Robinson, A.R.; Golnaraghi, M. The physical and dynamical oceanography of the Mediterranean. In *Ocean Processes in Climate Dynamics: Global and Mediterranean Examples*; Malanotte-Rizzoli, P., Robinson, A.R., Eds.; Springer: Dordrecht, The Netherlands, 1994; pp. 255–306. [CrossRef]
27. Bardají, T.; Goy, J.L.; Zazo, C.; Hillaire-Marcel, C.; Dabrio, C.J.; Cabero, A.; Ghaleb, B.; Silva, P.G.; Lario, J. Sea level and climate changes during OIS 5e in the Western Mediterranean. *Geomorphology* **2009**, *104*, 22–37. [CrossRef]
28. Incarbona, A.; Sprovieri, M.; Di Stefano, A.; Di Stefano, E.; Salvagio, D.; Pelosi, N.; Ribera, M.; Sprovieri, R.; Ziveri, P. Productivity modes in the Mediterranean Sea during Dansgaard-Oeschger (20,000–70,000 yr ago) oscillations. *Palaeogeogr. Palaeoclimatol. Palaeoecol.* **2013**, *392*, 128–137. [CrossRef]
29. POEM group. General circulation of the Eastern Mediterranean. *Earth Sci. Rev.* **1992**, *32*, 285–309. [CrossRef]
30. Millot, C. Circulation in Western Mediterranean. *J. Mar. Syst.* **1999**, *20*, 423–442. [CrossRef]
31. Millot, C.; Taupier-Letage, I. Circulation in the Mediterranean Sea. In *The Handbook of Environmental Chemistry*; Springer: Berlin/Heidelberg, Germany, 2005; Volume 5K, pp. 29–66. [CrossRef]
32. MEDCLIC. El Mar Mediterráneo. Available online: https://medclic.es/uploads/filer_public/7d/bf/7dbfe6a0-af47-44ff-990e-a07f25829229/u1_elmediterrani_medclic_cat.pdf (accessed on 13 June 2022).
33. Copernicus Marine Service. Mediterranean Sea Physics Reanalysis. *Dataset ID: MEDSEA_REANALYSIS_PHY_006_004.* Available online: https://marine.copernicus.eu (accessed on 21 June 2025).
34. CEAM/Meteoce; NOAA/NCEI. GHRSST Level 4 AVHRR_OI Global Blended Sea Surface Temperature Analysis v2.1 (GDS2). Available online: https://www.ncei.noaa.gov (accessed on 9 June 2025).
35. GretagMacbeth. *Munsell® Soil Color Charts, Revised Washable 2000 Edition*; GretagMacbeth: New Windsor, NY, USA, 2000; p. 10.
36. WoRMS. World Register of Marine Species. 2020. Available online: http://www.marinespecies.org/index.php (accessed on 19 August 2022).
37. Del Valle, L.; Fornós, J.J.; Pomar, F.; Pons, G.X.; Timar-Gabor, A. Aeolian-alluvial interactions at Formentera (Balearic Islands, Western Mediterranean): The late Pleistocene evolution of a coastal system. *Quat. Int.* **2020**, *566–567*, 271–283. [CrossRef]
38. Rose, J.; Meng, X.; Watson, C. Palaeoclimate and palaeoenvironmental responses in the western Mediterranean over the last 140 ka: Evidence from Mallorca, Spain. *J. Geol. Soc.* **1999**, *156*, 435–448. [CrossRef]
39. Andreucci, S.; Clemmensen, L.B.; Murray, A.; Pascucci, V. Middle Late Pleistocene coastal deposits of Alghero, northwestern Sardinia (Italy): Chronology and evolution. *Quat. Int.* **2010**, *222*, 3–16. [CrossRef]
40. Paskoff, R.; Sanlaville, P. *Les Côtes de la Tunisie: Variations du Niveau Marin depuis le Tyrrhenien*; Editions Maison de l'Orient: Lyon, France, 1983; p. 192.
41. Sheldon, N.D.; Tabor, N.J. Quantitative paleoenvironmental and paleoclimatic reconstruction using paleosols. *Earth-Sci. Rev.* **2009**, *95*, 1–52. [CrossRef]

42. Mauz, B.; Hijma, M.P.; Amorosi, A.; Porat, N.; Galili, E.; Bloemendal, J. Aeolian beach ridges and their significance for climate and sea level: Concept and insight from the Levant coast (East Mediterranean). *Earth-Sci. Rev.* **2013**, *121*, 31–54. [CrossRef]
43. Rodríguez-López, J.P.; Liesa, C.L.; Van Dam, J.; Lafuente, P.; Arlegui, L.; Ezquerro, L.; De Boer, P.L. Aeolian construction and alluvial dismantling of a fault-bounded intracontinental perspective on Late Pliocene climate change and variability. *Sedimentology* **2012**, *59*, 1536–1567. [CrossRef]
44. Polyak, V.J.; Onac, B.P.; Fornós JJHay, C.; Asmeron, Y.; Dorale, J.A.; Ginés, J.; Tuccimei, P.; Ginés, A. A highly resolved record of relative sea level in the western Mediterranean Sea during the last interglacial period. *Nat. Geosci.* **2018**, *11*, 860–864. [CrossRef]
45. Ferranti, L.; Antonioli, F.; Mauz, B.; Amorisi, A.; Dai Para, G.; Mastronuzzi, G.; Monaco, C.; Pappalardo, M.; Radtke, U.; Renda, P.; et al. Markers of the Last Interglacial Sea level highstand along the coast of Italy: Tectonic implications. *Quat. Int.* **2006**, *145–146*, 30–54. [CrossRef]
46. Andreucci, S.; Pascucci, V.; Murray, A.S.; Clemmensen, L.B. Late Pleistocene coastal evolution of san giovanni di Sinis, west Sardinia (Western Mediterranean). *Sediment. Geol.* **2009**, *216*, 104–116. [CrossRef]
47. Pascucci, V.; Sechi, D.; Andreucci, S. Middle Pleistocene to Holocene coastal evolution of NW Sardinia (Mediterranean sea, Italy). *Quat. Int.* **2014**, *328–329*, 3–20. [CrossRef]
48. Federici, P.R.; Pappalardo, M. Evidence of marine Isotope Stage 5.5 highstand in Liguria (Italy) and its tectonic significance. *Quat. Int.* **2006**, *145–146*, 68–77. [CrossRef]
49. Dumas, B.; Guérèmy, P.; Raffy, J. Evidence for sea-level oscillations by the "characteristic thickness" of marine deposits from raised terraces of Southern Calabria (Italy). *Quat. Sci. Rev.* **2005**, *24*, 2120–2136. [CrossRef]
50. Mauz, B. Late Pleistocene records of littoral processes at the Thyrrhenian Coast (Central Italy). Depositional environments and Luminsecence chronology. *Quat. Sci. Rev.* **1999**, *18*, 1173–1184. [CrossRef]
51. Mauz, B.; Fanelli, F.; Elmejdoub, N.; Barbieri, R. Coastal response to climate change: Mediterranean shorelines during the last interglacial (MIS 5). *Quat. Sci. Rev.* **2012**, *56*, 89–98. [CrossRef]
52. Alouane, M. Les Formations Quaternaires du Secteurs Littoraux du Maroc Septentrional (Régions de Tanger et de Nador): Analyse Morphostructurale, Lithostratigraphique et Sédimentologique. Ph.D. Thesis, Université Mohamed V-AGDAL, Rabat, Morocco, 2001; p. 206.
53. Occhietti, S.; Raynal, J.P.; Pichet, P.; Lefèvre, D. Aminostratigraphie des formations littorals Pléistocènes et holocènes de la region de Casablanca, Maroc. *Quaternaire* **2002**, *13*, 55–64. [CrossRef]
54. Jedoui, E.; Davaud, H.; Ismaïl, B.; Reyss, J.L. Analyse sédimentologique des d'epôts marins pléistocènes du Sud-Est tunisien: Mise en évidence de deux périodes de haut niveau marin pendant le sous-stade isotopique marin 5e (Eémien, Tyrrhénien). *Bull. Société Géologique Du Fr.* **2002**, *173*, 63–72.
55. Frechen, M.; Neber, A.; Tsatskin, A.; Boenigk, W.; Ronene, A. Chronology of Pleistocene sedimentary cycles in the Carmel coastal plain of Israel. *Quat. Int.* **2004**, *121*, 41–52. [CrossRef]
56. Jacobs, Z.; Roberts, D.L. Last Interglacial Age for aeolian and marine deposits and the Nahoon fossil human footprints, Southeast Coast of South Africa. *Quat. Geochronol.* **2009**, *4*, 160–169. [CrossRef]
57. Cawthra, H.C.; Jacobs, Z.; Compton, J.S.; Fisher, E.C.; Karkanas, P. Depositional and sea-level history from MIS 6 (Termination II) to MIS 3 on the southern continental shelf of South Africa. *Quat. Sci. Rev.* **2018**, *181*, 156–172. [CrossRef]
58. Hearty, P.J.; Neumann, A.C. Rapid Sea level and climate change at the close of the last Interglaciation (MIS 5e): Evidence from the Bahama Islands. *Quat. Sci. Rev.* **2001**, *20*, 1881–1895. [CrossRef]
59. Carew, J.L.; Mylroie, J.E. Quaternary carbonate eolianites of the Bahamas: Useful analogues for the interpretation of ancient rocks? In *Modern and Ancient Carbonate Eolianites*; Abegg, F.E., Harris, P.M., Loope, D.B., Eds.; SEPM Special Publication: Tulsa, OK, USA, 2008; Volume 71, pp. 33–45.
60. Hearty, P.J.; O'Leary, M.J. Carbonate aeolianites, quartz sands and Quaternary sea-level cycles, Western Australia: A chronostratigraphic approach. *Quat. Geochronol.* **2008**, *3*, 26–55. [CrossRef]
61. Sivan, D.; Gvirtzman, G.; Sass, E. Quaternary stratigraphy and paleogeography of the Galilee coastal plain, Israel. *Quat. Res.* **1999**, *51*, 280–294. [CrossRef]
62. Waelbroeck, C.; Labeyrie, L.; Michel, E.; Duplessy, J.C.; McManus, J.F.; Lambeck, K.; Balbon, E.; Labracherie, M. Sea-level and deep water temperature changes derived from benthonic foraminifera isotopic records. *Quat. Sci. Rev.* **2002**, *21*, 295–305. [CrossRef]
63. Rohling, E.J.; Grant, K.; Bolshaw, M.; Roberts, A.P.; Siddall, M.; Hemleben, C.; Kucera, M. Antarctic temperature and global sea level closely coupled over the past five glacial cycles. *Nat. Geosci.* **2009**, *2*, 500–504. [CrossRef]
64. Camoin, G.F.; Webster, J.M. Coral reef response to Quaternary sea-level and environmental changes: State of Science. *Sedimentology* **2015**, *62*, 401–428. [CrossRef]
65. Pappalardo, M.; Chelli, A.; Ciampalini, A.; Rellini, I.; Biagioni, F.; Brückner, H.; Fülling, A.; Firpo, M. Evolution of an upper Pleistocene aeolianite in the northern Mediterranean (Liguria, NW Italy). *Ital. J. Geosci.* **2013**, *132*, 290–303. [CrossRef]
66. Andreucci, S.; Pascucci, V.; Clemmensen, L.B. Upper Pleistocene coastal deposits of West Sardinia: A record of sea-level and climate change. *GeoActa* **2006**, *5*, 79–96.

67. Nathan, R.P.; Mauz, B. On the dose-rate estimate of carbonate-rich sediments for trapped charge dating. *Radiat. Meas.* **2008**, *43*, 14–25. [CrossRef]
68. Sivan, D.; Porat, N. Evidence from luminescence for Late Pleistocene formation of calcareous aeolianite (kurkar) and paleosol (hamra) in the Carmel Coast, Israel. *Palaeogeogr. Palaeoclimatol. Palaeoecol.* **2004**, *211*, 95–106. [CrossRef]
69. El-Asmar, H.M.; Wood, P. Quaternary shoreline development: The north-western coast of Egypt. *Quat. Sci. Rev.* **2000**, *19*, 1137–1149. [CrossRef]
70. Aiello, G.; Caccavale, M. Coasts on marine terraces of the Cilento Promontory: A try to add a brief correlation of your results, mainly based on MIS correlation. *Quat. Int.* **2024**, *in press*.
71. Savini, A.; Vertino, A.; Montagna, P.; Di Geronimo, I. Late Quaternary water depth and ecological conditions inferred from benthic foraminifera and sediment facies: A case study in the Western Mediterranean. *Water* **2021**, *13*, 480.
72. Sidall, M.; Rohling, E.J.; Almogi-Labin, A.; Hemleben, C.H.; Melscher, D.; Schmelzer, I.; Smed, D.A. Sea-level fluctuations during the last glacial cycle. *Nature* **2003**, *423*, 853–858. [CrossRef] [PubMed]
73. Rabineau, M.; Berné, S.; Olivet, J.L.; Aslanian, D.; Guillocheau, F.; Joseph, P. Paleo sea levels reconsidered from direct observation of paleoshoreline position during Glacial Maxima (for the last 500,000 yr). *Earth Planet. Sci. Lett.* **2006**, *252*, 119–137. [CrossRef]
74. Cutler, K.B.; Edwards, R.L.; Taylor, F.W.; Cheng, H.; Adkins, A.; Gallup, C.D.; Cutler, P.M.; Burr, G.S.; Bloom, A.L. Rapid sea-level fall and deep-ocean temperature change since the last interglacial period. *Earth Planet. Sci. Lett.* **2003**, *206*, 253–271. [CrossRef]
75. Polyak, V.J.; Onac, B.P.; Fornós, J.J.; Dorale, J.A.; Tuccimei, P. Evidence for stable sea-level during Marine Isotope Stage 5e of the Last Interglacial from the Western Mediterranean. In Proceedings of the AGU Meeting, San Francisco, CA, USA, 14 December 2014.
76. Martrat, B.; Grimalt, J.O.; Lopez-Martinez, C.; Cacho, I.; Sierro, F.J.; Flores, J.A.; Zahn, R.; Canals, M.; Curtis, J.H.; Hodell, D.A. Abrupt temperature changes in the western Mediterranean over the past 250,000 years. *Science* **2004**, *306*, 1762–1765. [CrossRef] [PubMed]
77. Martrat, B.; Grimalt, J.O.; Shackleton, N.J.; de Abreu, L.; Hutterli, M.A.; Stocker, T.F. Four climate cycles of recurring deep and surface water destabilizations on the Iberian margin. *Science* **2007**, *317*, 502–507. [CrossRef] [PubMed]
78. Pomar, F. Arquitectura i Facies Deposicionals de la Interferencia Entre la Sedimentació al·Luvial, col·Luvial i Eólica a les Illes Balears Durant el Pleistocè Superior: Implicacions Paleoclimàtiques. Ph.D. Thesis, Universitat de les Illes Balears, Palma, Spain, 2016; p. 375.
79. Zazo, C.; Goy, J.L. Sea-level changes in the Iberian Peninsula during the last 200,000 years. In *Late Quaternary Sea-Level Correlation and Applications*; Scott, D.B., Ed.; Kluwer Academic Publishers: Dordrecht, The Netherlands, 1989; pp. 27–39.
80. Vicens, D.; Pons, G.X. Registro fósil del Cuaternario litoral de Menorca. In *Geomorfología Litoral de Menorca: Dinámica, Evolución y Prácticas de Gestión*; Gómez-Pujol, L., Pons, G.X., Eds.; Societat d'Història Natural de les Balears: Palma, Spain, 2017; Volume 25, pp. 157–190.
81. Amorosi, A.; Antonioli, F.; Bertini, A.; Marabini, S.; Mastronuzzi, G.; Montagna, P.; Negri, A.; Rossi, V.; Scarponi, D.; Taviani, M.; et al. The Middle-Upper Pleistocene Fronte section (Taranto, Italy): An exceptionally preserved marine record of the Last Interglacial. *Glob. Planet. Change* **2014**, *119*, 23–28. [CrossRef]
82. Kindler, P.; Davaud, E.; Strasser, A. Tyrrhenian coastal deposits from Sardinia (Italy): A petrographic record of high sea levels and shifting climate belts during the last interglacial (isotopic substage 5e). *Palaeogeogr. Palaeoclimatol. Palaeoecol.* **1997**, *133*, 1–25. [CrossRef]
83. Chesi, F.; Delfino, M.; Abbazzi, L.; Carboni, S.; Lecca, L.; Rook, L. New fossil vertebrate remains from San Giovani de Sinis (Late Pleistocene, Sardinia): The last Mauremys (Reptilia, Testudines) in the Central Mediterranean. *Riv. Ital. Paleontol. Stratigr.* **2007**, *113*, 287–297. [CrossRef]
84. Marra, F.; Bahain, J.J.; Jicha, B.R.; Nomade, S.; Palladino, D.M.; Pereira, A.; Tolomei, C.; Voinchet, P.; Anzidei, M.; Aureli, D.; et al. Reconstruction of the MIS 5.5, 5.3 and 5.1 coastal terraces in Latium (central Italy): A re-evaluation of the sea-level history in the Mediterranean Sea during the last interglacial. *Quat. Int.* **2019**, *525*, 54–77. [CrossRef]
85. Meco, J.; Petit-Maire, N.; Fontugne, M.; Shimmield, G.; Ramos, A.J. The quaternary deposits in Lanzarote and Fuerteventura (Eastern Canary Islands, Spain): An overview. In *Climates of the Past, Proceedings of the CLIP Meeting, Lanzarote and Fuerteventura, Canary Islands, Spain, 2–7 June 1995*; Meco, J., Petit-Maire, N., Eds.; International Union Geological Sciences, UNESCO: Paris, France, 1997; pp. 123–136.
86. Roberts, N.; Jones, M.D.; Benkadjddour, A.; Eastwood, W.J.; Filippi, M.L.; Frogley, M.R.; Xai, H.F.; Leng, M.J.; Reed, J.M.; Stein, M.; et al. Stable isotope records of Late Quaternary Climate and hydrology fomr Mediterranean lakes: The ISOMED synthesis. *Quat. Sci. Rev.* **2008**, *27*, 2426–2441. [CrossRef]
87. Muhs, D.R.; Budahn, J.; Avila, A.; Skipp, G.; Freeman, J.; Patternson, D. The role of African dust in the formation of Quaternary soils on Mallorca, Spain and implications for the genesis of Red Mediterranean soils. *Quat. Sci. Rev.* **2010**, *29*, 2518–2543. [CrossRef]
88. Poole, A.J.; Shimmield, G.B.; Robertson, A.H.F. Late Quaternary uplift of the Troodos ophiolite, Cyprus: Uranium-series dating of Pleistocene coral. *Geology* **1990**, *18*, 894–897. [CrossRef]

89. Sivan, D.; Sisma-Ventura, G.; Greenbaum, N.; Bialik, O.M.; Williams, F.H.; Tamisiea, M.E.; Rohling, E.J.; Frumkin, A.; Avnaim-Katav, S.; Shtienberg, G.; et al. Eastern Mediterranean Sea levels through the last interglacial from a coastal-marine sequence in northern Israel. *Quat. Sci. Rev.* **2016**, *145*, 204–225. [CrossRef]
90. Gzam, M.; EL Mejdoub, N.; Jedoui, Y. Late quaternary sea level changes of Gabes coastal plain and shelf: Identification of the MIS 5c and MIS 5a onshore highstands, southern Mediterranean. *J. Earth Syst. Sci.* **2016**, *125*, 13–28. [CrossRef]
91. Galili, E.; Zviely, D.; Ronen, A.; Mienis, H.K. Beach deposits of MIS 5e high sea standas indicators for tectonic stability of the Carmel coastal plain, Israel. *Quat. Sci. Rev.* **2007**, *26*, 2544–2557. [CrossRef]

Disclaimer/Publisher's Note: The statements, opinions and data contained in all publications are solely those of the individual author(s) and contributor(s) and not of MDPI and/or the editor(s). MDPI and/or the editor(s) disclaim responsibility for any injury to people or property resulting from any ideas, methods, instructions or products referred to in the content.